Regulation of learning and memory by meningeal immunity: a key role for IL-4

Noël C. Derecki,[1,3] Amber N. Cardani,[1,4] Chun Hui Yang,[1] Kayla M. Quinnies,[1] Anastasia Crihfield,[1] Kevin R. Lynch,[2] and Jonathan Kipnis[1,3,4]

[1]Department of Neuroscience and [2]Department of Pharmacology, [3]Graduate Program in Neuroscience and [4]Graduate Program in Immunology, University of Virginia, Charlottesville, VA 22908

Proinflammatory cytokines have been shown to impair cognition; consequently, immune activity in the central nervous system was considered detrimental to cognitive function. Unexpectedly, however, T cells were recently shown to support learning and memory, though the underlying mechanism was unclear. We show that one of the steps in the cascade of T cell–based support of learning and memory takes place in the meningeal spaces. Performance of cognitive tasks led to accumulation of IL-4–producing T cells in the meninges. Depletion of T cells from meningeal spaces skewed meningeal myeloid cells toward a proinflammatory phenotype. T cell–derived IL-4 was critical, as IL-4$^{-/-}$ mice exhibited a skewed proinflammatory meningeal myeloid cell phenotype and cognitive deficits. Transplantation of IL-4$^{-/-}$ bone marrow into irradiated wild-type recipients also resulted in cognitive impairment and proinflammatory skew. Moreover, adoptive transfer of T cells from wild-type into IL-4$^{-/-}$ mice reversed cognitive impairment and attenuated the proinflammatory character of meningeal myeloid cells. Our results point to a critical role for T cell–derived IL-4 in the regulation of cognitive function through meningeal myeloid cell phenotype and brain-derived neurotrophic factor expression. These findings might lead to the development of new immune-based therapies for cognitive impairment associated with immune decline.

CORRESPONDENCE
Jonathan Kipnis:
kipnis@virginia.edu

Abbreviations used: ANOVA, analysis of variance; BDNF, brain-derived neurotrophic factor; CNS, central nervous system; CSF, cerebrospinal fluid; MWM, Morris water maze; qRT-PCR, quantitative real-time PCR; SCID, severe combined immune deficient; UBC, ubiquitin C.

Immune activity in the central nervous system (CNS) is restricted, primarily because of the blood–brain barrier (Hickey, 1999; Pachter et al., 2003; Carson et al., 2006; Bechmann et al., 2007). Nevertheless, a substantial body of research has addressed pro- and antiinflammatory cytokine activity in CNS functioning. Sickness, stress, depression, aging, and other somatic conditions that detrimentally affect cognitive function have been linked to an increase in the expression of proinflammatory cytokines and their receptors in different areas of the brain (Dantzer, 2001, 2008; Reichenberg et al., 2001; Kelley et al., 2003). One such area is the hippocampus, which is partially responsible for spatial learning and memory acquisition (O'Keefe and Dostrovsky, 1971; Griffin et al., 2007). Cytokines principally shown to have a detrimental effect on cognitive function include TNF, IL-1β, IL-6, and IL-12 (Sparkman et al., 2006; Baune et al., 2008; McAfoose et al., 2009). Innate immune cells, both peripheral and CNS resident, were proposed as the source of proinflammatory cytokines that are secreted in response to any deviation from physiological homeostasis as a result of stress, disease, or injury (Perry et al., 2007). Adaptive immunity has been less well studied. Interestingly, IL-4 was shown to mediate numerous beneficial effects on CNS function in animal models of aging brain and Alzheimer's disease (Lyons et al., 2007; Clarke et al., 2008; Cao et al., 2009; Loane et al., 2009).

Studies from our own and other laboratories have shown that the adaptive arm of the immune system plays a major role in the functioning of the normal brain and regulates cognitive function (Kipnis et al., 2004; Brynskikh et al., 2008). Specifically, we found an association between adaptive immune deficiency and reduced cognitive abilities in spatial learning and memory tasks. When T cell–deficient mice were injected with splenocytes from wild-type

The Rockefeller University Press $30.00
J. Exp. Med. Vol. 207 No. 5 1067-1080
www.jem.org/cgi/doi/10.1084/jem.20091419

counterparts, their performance on learning and memory tasks significantly improved (Kipnis et al., 2004). Injection of T cell–deficient mice with T cell–depleted splenocytes did not affect their performance, indicating that cognitive improvement was T cell dependent (Brynskikh et al., 2008). A recent study showed that acute depletion of T cells by administration of anti-CD3 antibodies results in cognitive impairment within 5 d, and that the effect is mediated by $CD4^+$ but not $CD8^+$ T cells (Wolf et al., 2009).

Although the function of the healthy brain is affected by the immune system (Kipnis et al., 2004; Ziv et al., 2006), under normal physiological conditions no T cells are found in the CNS parenchyma. However, the brain and spinal cord are surrounded by a multipartite membranous covering—the meninges—comprising an outer dura mater, intermediate arachnoid mater, and inner pia mater. Cerebrospinal fluid (CSF), produced by choroid plexus epithelia, flows within the confines of the meninges (Cserr and Knopf, 1992; Ransohoff et al., 2003). CSF drains into cervical lymph nodes (Widner et al., 1988), enabling peripheral T cells to respond to CNS antigens under certain pathological conditions. Thus, although immune cell access to the CNS parenchyma of the healthy brain is restricted, access to the meninges and choroid plexus is more feasible. Accordingly, the meninges and choroid plexus are heavily populated by myeloid cells, as well as by substantial numbers of T cells (Qing et al., 2000; Kivisäkk et al., 2003; Rosicarelli et al., 2005). It is therefore plausible that neuroimmune interactions affecting learning and memory originate in the meninges and choroid plexus/ventricular areas rather than in the parenchyma. With this in mind, we decided to examine the possibility that T cell function in the meningeal spaces is a prerequisite for the role of these cells in learning and memory.

In this paper we show that in wild-type mice trained in a spatial learning and memory task, the Morris water maze (MWM), IL-4–producing T cells accumulate in meningeal spaces. Acute depletion of T cells from meningeal spaces results in impairment of learning and memory, and the appearance of a skewed proinflammatory phenotype of meningeal myeloid cells. Strikingly, IL-$4^{-/-}$ mice exhibited a skewed proinflammatory meningeal myeloid phenotype and cognitive impairment reminiscent of that seen in T cell–depleted mice, and was reversed by injection of wild-type T cells. Moreover, transplantation of bone marrow from IL-$4^{-/-}$ mice into irradiated wild-type mice resulted in cognitive impairment and proinflammatory meningeal myeloid skew reminiscent of that seen in IL-$4^{-/-}$ mice, linking meningeal T cell–derived IL-4 to meningeal myeloid cell phenotype and cognitive function. The regulation of brain-derived neurotrophic factor (BDNF) as a possible mechanism underlying the beneficial role of T cell–derived IL-4 is shown.

RESULTS

Acute suppression of T cells results in impairment of learning and memory

Several genetically immunodeficient mouse strains have previously been shown to exhibit severe cognitive impairment when examined on tests of spatial learning and memory (Kipnis et al., 2004; Brynskikh et al., 2008). We were interested to see if immunosuppressive drugs, currently in clinical trials or used in disease treatment, would yield a similar phenotype of cognitive impairment. To that end, wild-type mice were treated daily by oral administration of 1 mg/kg FTY720, a compound that causes internalization of the sphingosine 1-phosphate receptor 1 on thymocytes and lymphocytes, thus sequestering these cells in lymph nodes and inducing peripheral lymphopenia (Brinkmann et al., 2002; Yang et al., 2003; Kharel et al., 2005).

To examine whether acute T cell depletion would impair learning and memory, we treated animals daily with an oral administration of 1 mg/kg FTY720 starting 1 wk before the initiation of training in the MWM spatial learning and memory task. Animals were continued on FTY720 treatment throughout training. FTY720-treated mice took significantly longer to find the hidden platform during the acquisition phase (the average of all four trials per day is presented; Fig. 1 a, i). When the platform was removed for the probe trial (removal of the platform is intended to test the strength of the acquired memory, and thus the percentage of time spent by mice in the quadrant where the platform was originally located is calculated), FTY720-treated mice spent significantly less time in the training quadrant than control mice (Fig. 1 a, ii). To further characterize memory deficits of FTY720-treated mice, we also examined the number of crossings the mice made through a circular area circumscribing the original platform location and the time required for the first crossing of this area. FTY720-treated mice fared significantly worse on both of these parameters (Fig. 1 a, iii and iv) than controls. On the reverse trial, when the platform was placed in the quadrant opposite to the original, PBS-treated mice exhibited normal learning within the 2 d, whereas the learning of FTY720-treated mice was significantly attenuated (the average of each individual trial is presented to follow the improvement in the performance; Fig. 1 a, v). No difference between the groups was evident in the visible platform task performed on day 8 (not depicted), suggesting no difference in motor function, vision, or motivation to escape the water.

At the end of MWM training, peripheral immunity was examined. As expected, lymphocyte levels in circulating blood were significantly reduced in FTY720-treated as compared with PBS-treated mice (Fig. S1).

To support the notion that FTY720's effect was through suppression of the immune response, we treated severe combined immune-deficient (SCID) mice with FTY720 in a regimen identical to that used for wild-type mice (1 mg/kg starting 1 wk before the initiation of training in the MWM). SCID mice performed poorly on the MWM, as was expected from previous studies (Kipnis et al., 2004; Brynskikh et al., 2008), and treatment with FTY720 did not affect their performance (Fig. 1 b).

To eliminate T cells from meningeal spaces instead of creating peripheral lymphopenia, we used anti-VLA4 antibodies that have previously been shown to be effective in their inhibition of T cell migration into the CNS (Yednock et al., 1992).

Animals were given three i.p. injections of 1.2 mg anti-VLA4 per mouse (or the same amount of rat IgG for control mice) 5 d before the beginning of MWM, 1 d before the training, and after 4 d of training. Anti-VLA4–treated mice took significantly longer to find the hidden platform during the acquisition phase (Fig. 1 c, i). When the platform was removed for the probe trial, anti-VLA4–treated mice spent significantly less time in the training quadrant than control mice (Fig. 1 c, ii). The number of crossings of the original platform location made by control mice were significantly higher than those made by anti-VLA4–treated mice (Fig. 1 c, iii). Finally, the latency for anti-VLA4–treated mice to first cross the original location of the platform was significantly greater than that of control mice (Fig. 1 c, iv). On the reverse trial, control mice exhibited normal learning within the 2 d, whereas the learning of anti-VLA4–treated mice was significantly attenuated (Fig. 1 c, v). No difference between the groups was evident in the visible trial (not depicted).

To address the possible differential effect of long- vs. short-term treatment with these drugs, we treated animals with either 4.3×10^{-3} mg/ml FTY720 in drinking water or injected them with 1.2 mg anti-VLA4 per mouse two times a week over a period of 8 wk. Two control mouse groups were used: rat IgG treated (at the same volume/frequency) and untreated. Both groups of control mice were identical and were combined for the ease of presentation. Both groups of treated mice exhibited substantial cognitive impairment, as examined in the MWM task (Fig. 1 d). Treated groups took significantly longer to find the hidden platform during the acquisition phase (Fig. 1 d, i). In a probe trial, control mice spent significantly more time in the training quadrant as compared with the anti-VLA4–treated group (Fig. 1 d, ii). The number of crossings of the original platform location made by control mice were significantly higher than those made by FTY720-treated mice (Fig. 1 d, iii). Finally, the latency for the treated mice to first cross the original location of the platform was significantly greater in both treated groups than that of control (Fig. 1 d, iv). On the reverse trial, control mice exhibited normal learning within the 2 d, whereas the learning of anti-VLA4– and FTY720- treated mice was significantly attenuated (Fig. 1 d, v). No difference between the groups was evident in the visible platform trial (not depicted).

To examine the effects of immune suppression on performance in a brief learning and memory task with minimal time given to training, in which an immunological response could not be generated, we compared control and FTY720-treated mice (1 mg/kg for 8 d before the examination) in contextual fear conditioning, an assay requiring only brief training (one 10-min training session). FTY720-treated mice did not show any difference in freezing behavior within the training context as compared with their control counterparts (Fig. 1 e), suggesting that in a temporally truncated learning and memory task, wherein a salient immune response cannot be built within the time frame, a lack of T lymphocytes does not affect learning behavior.

Meningeal T cell response after MWM learning and memory task performance

In an attempt to better understand the cellular and molecular mechanisms underlying the observed beneficial effect of T cells on performance in the MWM, we examined T cell response after task performance. Immunohistological examination of brain tissue did not reveal any T cells in brain parenchyma from either naive or MWM-trained mice. However, T cells were prominently evident in meningeal areas: subarachnoid spaces (Fig. 2 a), ventricle walls, and choroid plexus (not depicted). Meningeal contents of T cells were quantified by stereological counting of $CD3^+$ cells in coronal slices. A significant increase in $CD3^+$ cells was evident in the meninges of mice that underwent training in the MWM task (Fig. 2 b). To substantiate these results, single-cell suspensions of meningeal tissue from control and MWM-trained mice were prepared and examined by FACS. The series of gates that allow reliable identification of the population of meningeal T cells is illustrated in Fig. 2 c (see Materials and methods). A substantial increase in $CD3^+CD4^+$ cell numbers was evident in meninges of MWM-trained as compared with control mice (Fig. 2 c, iv). From FACS data we extrapolated the total numbers of $CD4^+$ and $CD8^+$ T cells in the meninges of naive and trained wild-type mice. A significant increase in $CD4^+$ but not $CD8^+$ T cell numbers after training is evident (Fig. 2 d). Numbers obtained using this calculation method were similar to those obtained by stereological counting (Fig. 2 a) but slightly higher, likely because of the fact that the entirety of the meninges, including meningeal tissue surrounding the cerebellum and olfactory bulbs of the brain, is used in FACS.

To further characterize T cells from naive and MWM-trained wild-type mice, we examined their activation phenotype. A substantial increase in CD69-expressing meningeal $CD4^+$ T cells was evident after training, whereas meningeal $CD8^+$ T cells did not show induction of the early activation marker CD69 (Fig. 2 e). Because only $CD4^+$ T cells had been activated in response to task performance and this is the major T cell population in the meninges (Fig. 2 d), we concentrated on this population. We also examined expression of the CD25 activation marker on $CD4^+$ T cells. To exclude the population of naturally occurring regulatory T cells constitutively expressing CD25, the negative fraction of Foxp3-labeled cells was examined for CD25 expression. Indeed, meningeal cells from MWM-trained mice showed an increase in $CD4^+Foxp3^-CD25^+$ cells (Fig. 2 f). Next, T cells were examined for intracellular cytokine profile. A striking induction in IL-4–producing $CD4^+$ T cells was revealed in the meninges of MWM-trained mice, whereas IFN-γ–producing T cells were not substantially changed after MWM training (Fig. 2 g).

We examined meningeal immunity after treatment with FTY720 or anti-VLA4. With FTY720 treatment, $CD4^+$ T cells in the meninges were dramatically reduced in numbers (Fig. 2 h). The presented populations were gated for $CD45^+$ and $CD3^+$ and then examined for CD4 expression. Although a massive general reduction in all T cells was evident (Fig. 2 h),

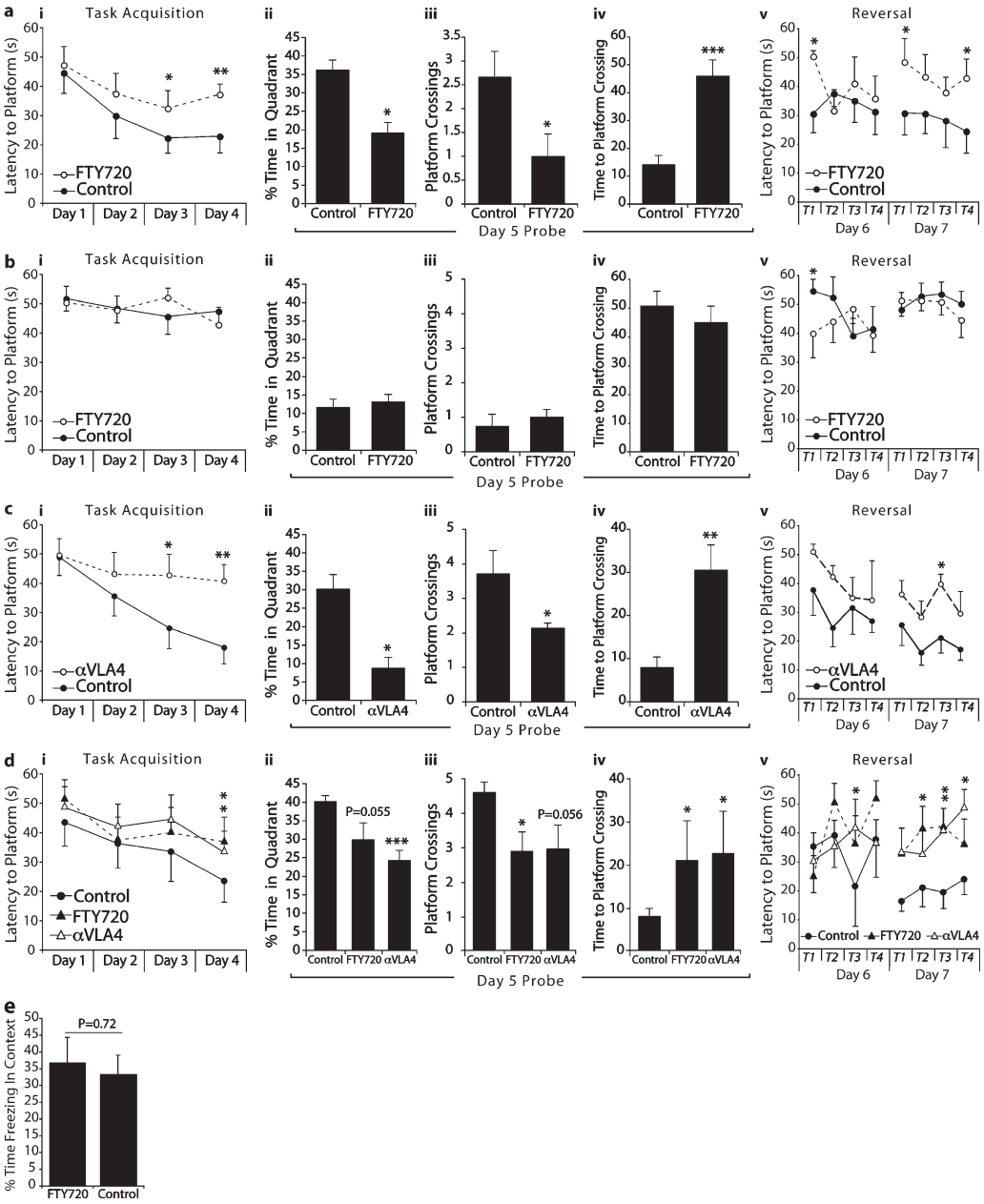

Figure 1. Depletion of T cells is correlated with impairment of learning and memory in the MWM task. All behavior experiments were performed by an experimenter blinded to the identity of the experimental groups and were recorded with the EthoVision video tracking system. Representative experiments are shown out of at least two to three independently performed in each case. (a, i–v) PBS- (control) and FTY720-treated mice of an identical genetic background (BALB/c) were monitored during the MWM task. During the acquisition (i) and reversal (v) phases of the task, FTY720-treated mice took significantly longer than controls to locate the hidden platform. Two-way repeated measures ANOVA was used for statistical analysis (*, $P < 0.05$ for overall acquisition; **, $P < 0.01$ for reversal day 2). The Bonferroni post-hoc test was used for individual pair comparisons ($n = 8–9$ mice/group; *, $P < 0.05$; **, $P < 0.01$). A probe trial was performed on day 5, and the percentage of time spent in the training quadrant (ii), the number of times each mouse passed over a circular space circumscribing the location of the original platform (iii), and the latency to reach the original platform location (iv) were recorded. FTY720-treated mice showed significantly reduced time spent in the training quadrant (ii), passed over the original platform location fewer times (iii), and took significantly longer to successfully locate the original platform location (iv; Student's *t* test; *, $P < 0.05$; ***, $P < 0.001$). (b, i–v) Control and FTY720-treated SCID mice of an identical genetic background (BALB/c) were monitored during the MWM task. No differences were seen in either the acquisition (i) or reversal phase (v). A probe trial was performed on day 5, and the percentage of time spent in the training quadrant (ii), the number of times each mouse passed over a circular space circumscribing the location of the original platform (iii), and the latency to reach the original platform location (iv) were recorded. FTY720-treated SCID mice did not differ from control SCID mice in time spent in any of the these measures (*, $P < 0.05$; $n = 8–9$ mice/group). (c, i–v) Control and anti-VLA4–treated mice of an identical genetic background (BALB/c) were monitored during the MWM task. During the acquisition (i) and reversal (v) phases of the task, anti-VLA4–treated mice took significantly longer than controls to locate the

when the CD4+ T cells from control and FTY720-treated meninges were examined for memory/naive cell markers, naive CD62L+ and/or CD44lo cells were clearly the most affected by FTY720 treatment (Fig. 2 i). Treatment with an antibody to VLA4 eliminated a majority of CD4+ T cells from the meninges (Fig. 2 j), with memory cells, expressing high levels of CD44, affected more than others (Fig. 2 k).

Meningeal myeloid cell response after cognitive task performance and its T cell–dependent regulation

In addition to T cells, the meninges are also well populated by myeloid cells. Micrographs of choroid plexus demonstrate CD68+ cells (myeloid origin) expressing MHCII (Fig. 3 a). These cells are representative of those observed in subarachnoid spaces and in ventricular walls (not depicted), i.e., throughout the meninges. Given the observed changes in meningeal T cells upon MWM training we reasoned that concomitant changes might be apparent in the meningeal myeloid population. Indeed, a substantial induction in activated myeloid cells (CD69+) was evident in the meninges of mice after MWM task performance (Fig. 3 b).

To address the possibility that T cells might be involved in the regulation of the phenotype of meningeal myeloid cells, we examined their expression of proinflammatory cytokines upon acute depletion of meningeal T cells using either FTY720 or anti-VLA4 antibody treatment. CD11b+ cells isolated from the meninges of FTY720- or anti-VLA4–treated mice exhibit higher levels of the proinflammatory cytokines TNF and/or IL-12 (Fig. 3, c and d), suggesting that in the absence of T cells, meningeal myeloid cells acquire a skewed proinflammatory phenotype in response to cognitive task performance.

To further support this hypothesis, we examined the cytokine profile of meningeal myeloid cells from wild-type and SCID mice (lacking both T and B lymphocytes) after MWM training. Meningeal myeloid cells from SCID mice expressed significantly higher levels of TNF and IL-12 than those from wild-type mice (Fig. 3 e). Moreover, we compared meningeal immunity in control SCID mice and SCID mice repopulated with T cells. SCID mice were injected i.p. with 20×10^6 CD3+ T cells isolated from syngeneic wild-type or IL-4$^{-/-}$ mice or with PBS (control), and after 2 wk were trained in the MWM. CD4+ T cells were found in meningeal isolates of T cell–injected mice (Fig. 3 f), and meningeal myeloid cells obtained from mice injected with wild-type T cells exhibited lower numbers of TNF-producing CD11b+ cells than PBS-injected counterparts (Fig. 3 g). IL-4$^{-/-}$ T cells were also found in the meningeal spaces of SCID recipients (Fig. 3 f); however, they did not affect the proinflammatory skew of meningeal myeloid cells (Fig. 3 g).

Analysis of the aforementioned meningeal myeloid cells was based on a series of gates applied to all samples, as indicated in Fig. 3 h, using a viability dye (live/dead gate for the elimination of dead cells; i), side/forward scatter (scatter gate for the elimination of cell debris; ii), CD45 versus event count (leukocyte gate for the identical number of analyzed leukocytes; iii), pulse width (singlets gate for the elimination of cell aggregates; iv), and CD11b, a myeloid cell marker (a myeloid gate; 3×10^3 myeloid cells were analyzed from each sample as indicated; v).

The essential role of IL-4 in the regulation of meningeal myeloid cells and in cognitive task performance

To further address the role of T cell–derived IL-4 in the regulation of meningeal myeloid cell phenotype and, in turn, of cognitive function, we examined IL-4$^{-/-}$ mice in terms of their MWM task performance. IL-4$^{-/-}$ mice exhibited an astonishingly severe phenotype of impaired cognitive function when compared with their wild-type controls. IL-4$^{-/-}$ mice took significantly longer to find the hidden platform during the acquisition phase (Fig. 4 a, i). In the probe trial, IL-4$^{-/-}$ mice spent significantly less time in the training quadrant than control mice (Fig. 4 a, ii). To further characterize memory deficits of IL-4$^{-/-}$ mice, we also examined the number of crossings of the original location of the platform and the time required for the first crossing that the mice made to the original platform location. IL-4$^{-/-}$ mice fared significantly worse on both parameters measured than did their wild-type counterparts (Fig. 4 a, iii and iv). On the reverse trial, IL-4$^{-/-}$ mice also exhibited a remarkable impairment (Fig. S2). No difference between the groups was evident in the visible platform trials (not depicted).

To link the cognitive impairment seen in IL-4$^{-/-}$ mice with meningeal immunity, we examined meningeal myeloid

hidden platform. Two-way repeated measures ANOVA was used for statistical analysis (*, $P < 0.05$; and **, $P < 0.01$ for both acquisition and reversal). The Bonferroni post-hoc test was used for individual pair comparisons ($n = 8$ mice/group; *, $P < 0.05$; **, $P < 0.01$). During the probe trial, anti-VLA4–treated mice showed significantly reduced time spent in the training quadrant (ii), passed over the original platform location fewer times (iii), and took significantly longer to successfully locate the original platform location (iv; Student's *t* test; *, $P < 0.05$; **, $P < 0.01$). (d, i–v) Control and long-term FTY720- and anti-VLA4–treated mice of an identical genetic background (BALB/c) were monitored during the MWM task. During the acquisition (i) and reversal (v) phases of the task, both FTY720- and anti-VLA4–treated mice took significantly longer than controls to locate the hidden platform. Two-way repeated measures ANOVA was used for statistical analysis (*, $P < 0.05$; and **, $P < 0.01$ for both acquisition and reversal). The Bonferroni post-hoc test was used for individual pair comparisons ($n = 6$–7 mice/group; *, $P < 0.05$). During the probe trial, anti-VLA4–treated mice showed significantly reduced time spent in the training quadrant (iii) and took significantly longer to successfully locate the original platform location (iv). FTY70-treated mice passed over the original platform location fewer times (ii) and took significantly longer to successfully locate the original platform location (iv; Student's *t* test; *, $P < 0.05$; ***, $P < 0.001$). (e) Mice were placed in a conditioning context for 2 min before receiving five tone/shock pairings spaced by 1-min inter-trial intervals. 48 h later the mice received a 5-min test in the training context. Freezing was scored via an automated system during all sessions and used as an index of memory. No differences were seen between control and FTY720-treated mice. Error bars represent SEM.

cells for cytokine expression. A significant increase in pro-inflammatory cytokine production (TNF) by meningeal myeloid cells from IL-4$^{-/-}$ mice was evident as compared with myeloid cells from the meninges of wild-type counterparts (Fig. 4 b). To substantiate that the results shown in meninges by FACS were relevant to areas in the CNS involved in spatial learning and memory, we also looked at levels of mRNA for TNF in hippocampi from MWM-trained wild-type and IL-4$^{-/-}$ mice by quantitative real-time PCR (qRT-PCR). Hippocampi from MWM-trained IL-4$^{-/-}$ mice showed significantly higher levels of TNF mRNA (Fig. 4 c). No neurodevelopmental abnormalities were found in IL-4$^{-/-}$ mouse brain gross anatomy compared with wild-type counterparts (Fig. S3).

To link the observed results to the effects of immune-derived IL-4, we undertook the following experiments. First, bone marrow transplantation from IL-4$^{-/-}$ mice to irradiated wild-type recipients was performed. 40 d after bone marrow transplantation, mice were examined for their performance in the MWM. A significant but partial (compared with IL-4$^{-/-}$ mice) impairment in MWM task performance was evident in IL-4$^{-/-}$ bone marrow recipients as compared with control counterparts that received bone marrow from wild-type mice. Mice that received bone marrow from IL-4$^{-/-}$ donors took significantly longer to find a hidden platform than controls (Fig. 4 d, i). In the probe trial, IL-4$^{-/-}$ bone marrow recipient mice spent less time in the training quadrant than control mice, albeit no statistical significance was observed in this particular measurement (Fig. 4 d, ii). To further characterize memory deficits of IL-4$^{-/-}$ bone marrow recipient mice, we examined the number of crossings of the original location of the platform and the time required for the

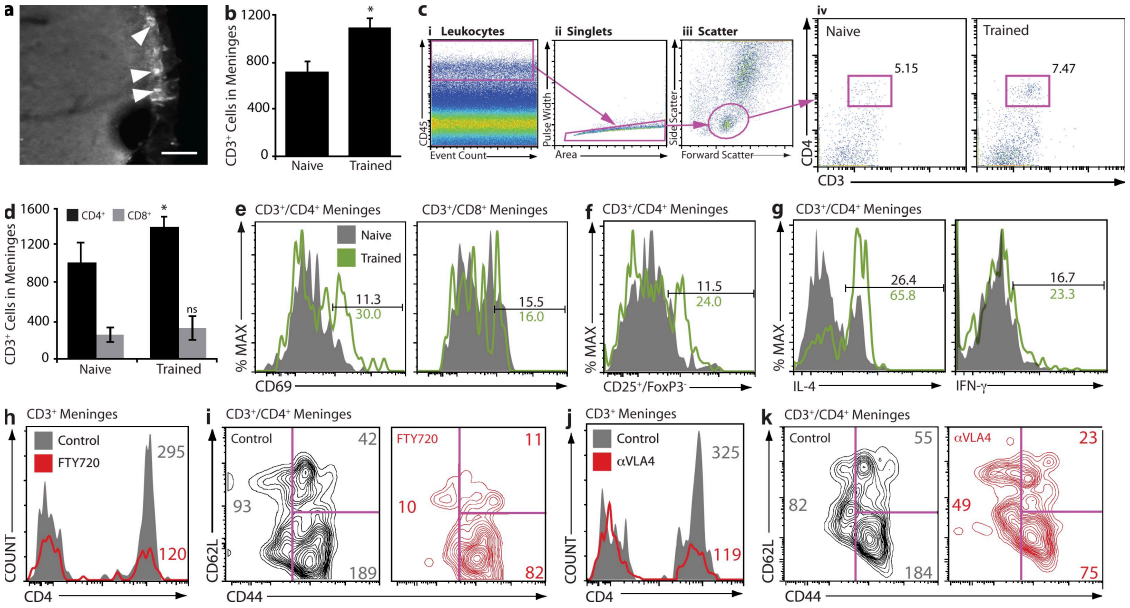

Figure 2. Accumulation and activation of IL-4–producing T cells in the meningeal spaces of MWM-trained mice. (a and b) Whole brain cryosections were labeled for CD3. Subarachnoid spaces occupied by CD3$^+$ cells are presented, and arrowheads point to CD3$^+$ cells. Bar, 50 µm (a). CD3$^+$ cells were stereologically counted. A significant increase in CD3$^+$ cells was found in trained mice (b). (c, i–iii) Meningeal single-cell suspensions were examined by FACS for CD3$^+$/CD4$^+$ cells in naive and MWM-trained mice. In each sample, 10^4 CD45^{hi} events were examined (i); CD45^{hi} events were gated by scatter (ii), and CD4 versus CD3, revealing an increase in CD4$^+$ T cells in the meninges of trained mice (iii). Experiments were performed three separate times with meninges pooled from four mice with similar results. The FACS plot shown is representative (c, iv). (d) The entirety of one single sample from each group (naive or MWM-trained) was read by FACS and normalized to one another by CD45^{hi} count and gated on CD3, CD4, and CD8. The numbers of CD3$^+$/CD4$^+$ and CD3$^+$/CD8$^+$ cells obtained from each sample were multiplied by the total number of samples prepared from the group and divided by four (the number of mice in the group) to arrive at a representative CD4$^+$ and CD8$^+$ T cell count per single mouse meninges. Meningeal preparations from MWM-trained mice displayed significantly higher numbers of CD4$^+$ but not CD8$^+$ T cells than meningeal preparations from naive mice. Error bars represent SEM. (e and f) CD3$^+$ cells from meninges of naive and MWM-trained mice were examined for expression of the activation markers CD69 and CD25, and the cytokines IL-4 and IFN-γ. CD4$^+$ but not CD8$^+$ cells from MWM-trained mice showed approximately threefold up-regulation in expression of CD69 (e) and similar up-regulation in effector (Foxp3$^-$) T cells expressing CD25 (f) as compared with cells from naive mice. Cells from MWM-trained mice also showed a substantial increase in intracellular expression of IL-4 but not IFN-γ as compared with naive animals (g). (h–k) FACS analysis of meningeal isolates from MWM-trained FTY720-treated and control mice (h and i), and anti-VLA4–treated and control mice (j and k). Analysis of CD3$^+$ cells from meninges of FTY720-treated mice indicates a reduction in meningeal CD4$^+$ T cells as compared with controls; numbers indicate cell counts and reflect the analyzed sample rather than the content of the entire meningeal isolation (h); a specific reduction in CD44^{lo}CD62L$^+$ (T_{Naive}) subpopulation in FTY720-treated mice is presented (i). Anti-VLA4–treated mice exhibit reduction in meningeal CD4$^+$ T cells as compared with controls (j), particularly the subpopulation characterized by the CD44^{hi}/CD62L$^-$ ($T_{Effector\ Memory}$) phenotype (k). At least two independent experiments with at least four mice in each group were performed. Results from independent experiments are shown. Numbers indicate percentages.

first crossing that the mice made to the original platform location. IL-4$^{-/-}$ bone marrow recipients fared significantly worse on both parameters measured than did controls (Fig. 4 d, iii and iv). Examination of meningeal myeloid cells from these two groups of mice revealed a marked proinflammatory skew in meningeal myeloid cells of mice that received bone marrow from IL-4$^{-/-}$ mice as compared with wild-type bone marrow recipients (Fig. 4 e).

In an additional experiment, IL-4$^{-/-}$ mice were injected i.p. with 20 × 10^6 T cells from either wild-type mice expressing GFP under the ubiquitin C (UBC) promoter (i.e., injected T cells are GFP$^+$) or IL-4$^{-/-}$ donors and were tested 2 wk later in the MWM. Although IL-4$^{-/-}$ T cells did not affect the MWM performance of IL-4$^{-/-}$ mice, injection of these mice with T cells from wild-type donors significantly improved their performance in the MWM task (Fig. 4 f). Wild-type T cell–injected IL-4$^{-/-}$ mice took significantly less time to find a hidden platform than IL-4$^{-/-}$ T cell–injected controls (Fig. 4 f, i). In the probe trial, mice injected with wild-type T cells spent significantly more time in the training quadrant than mice injected with IL-4$^{-/-}$ T cells (Fig. 4 f, ii). Moreover, on the additional two memory parameters—the number of crossings of the original location of the platform and the time required for the first crossing that the mice made to the original platform location—mice injected with T cells from wild-type mice exhibited significantly better function than mice injected with IL-4$^{-/-}$ T cells (Fig. 4 f, iii and iv). Examination of meningeal myeloid cells from these two groups of mice revealed that mice injected with wild-type T cells demonstrated a striking amelioration of the proinflammatory meningeal myeloid skew characteristic to IL-4$^{-/-}$ mice (Fig. 4 g). In contrast, injection of IL-4$^{-/-}$ recipients with IL-4$^{-/-}$ T cells did not affect meningeal myeloid cell phenotype (Fig. 4 g). Meningeal isolates from IL-4$^{-/-}$ mice that received GFP$^+$ T cells were also labeled extracellularly for CD3 and CD4, and intracellularly for IFN-γ and IL-4. GFP$^+$ (wild-type, transferred) and GFP$^-$ (endogenous) CD4$^+$ T cells were compared for expression of

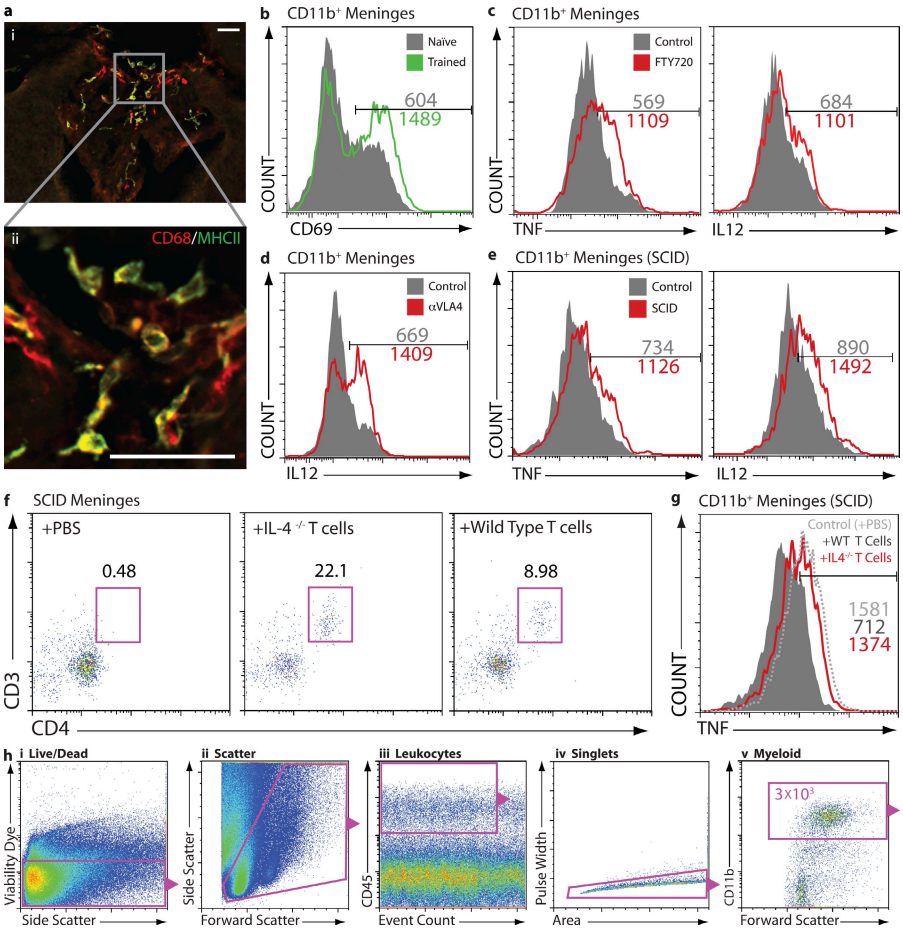

Figure 3. T cell–dependent regulation of meningeal myeloid cell phenotype in MWM-trained mice. (a) Whole brain cryosections were double labeled for CD68 and MHCII. Positive cells (myeloid) in the choroid plexus of the third ventricle are presented. Bars, 50 µm. (b–e) FACS analyses were performed at least three times independently with at least three to four mice in each group. Numbers on histograms indicate actual cell counts. CD11b$^+$ cells from meninges of MWM-trained animals display a marked increase in the expression of CD69 as compared with naive animals (b). CD11b$^+$ cells from the meninges of acutely immunosuppressed FTY720-treated animals show a proinflammatory skew as measured by TNF and IL-12 expression (c). Anti-VLA4–treated animals display an increase in the expression of the proinflammatory cytokine IL-12 in meningeal myeloid cells (d). CD11b$^+$ cells from the meninges of chronically immunodeficient SCID mice display a proinflammatory skew in comparison to controls, as measured by TNF and IL-12 expression (e). (f and g) SCID mice injected i.p. with PBS, 2 X 10^6 T lymphocytes from IL-4$^{-/-}$ mice, or 2 X 10^6 T lymphocytes from wild-type mice. At least six mice in each group were analyzed in two independent experiments. Plots depict CD3$^+$/CD4$^+$cells isolated from the meninges of transfused SCID mice (numbers indicate percentages; f). Histograms show TNF expression as measured by FACS analysis of meningeal cells expressing CD11b. CD11b$^+$ cells from the meninges of SCID mice transfused with wild-type T cells showed a reduction in proinflammatory cytokine production, and SCID mice transfused with T cells from IL-4$^{-/-}$ mice showed no such reduction (g). (h) Representative labeling and gating scheme for meningeal myeloid cells in b–e and g by FACS is presented. Viable cells as determined by a live/dead gate (i), forward and side scatter to eliminate debris (ii), CD45^{hi} cells to eliminate possible microglial contamination (iii), and single-cell selection as determined by pulse width versus area gate (iv), CD11b$^+$ gate. CD45/event count gates were adjusted to yield identical numbers (3 X 10^3) of myeloid-derived cells in each sample.

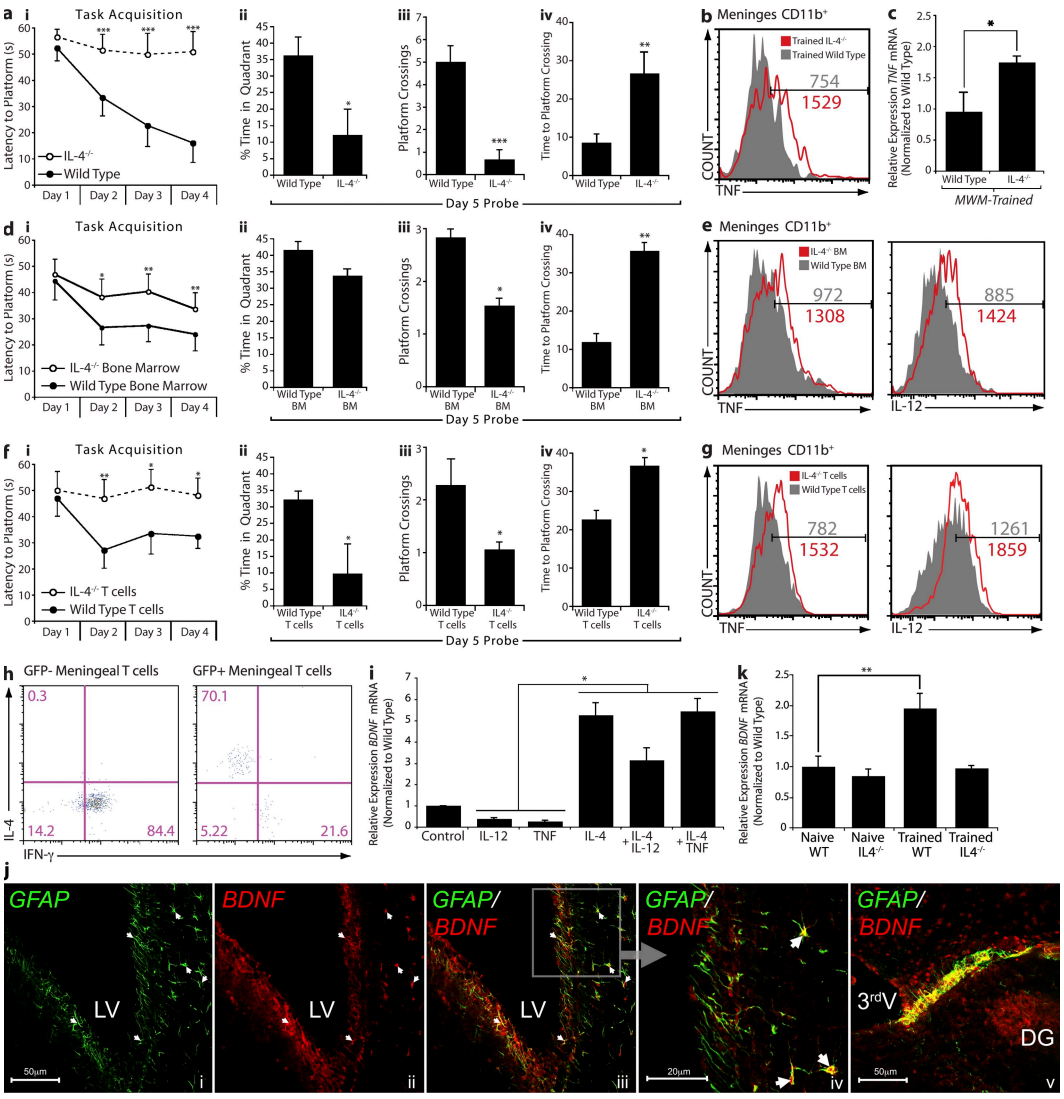

Figure 4. T cell–derived IL-4 regulates meningeal myeloid cell phenotype and influences learning and memory. All behavior experiments were performed by an experimenter blinded to the identity of experimental groups and were recorded with the EthoVision video tracking system. Representative experiments are shown out of at least two to three independently performed in each case. (a, i–iv) Control and IL-4$^{-/-}$ mice of identical genetic background (C57BL/6J) were monitored during the MWM task performance. During the acquisition (i) phase of the task, IL-4$^{-/-}$ mice took significantly longer than controls to locate the hidden platform. Two-way repeated measures ANOVA was used for statistical analysis (***, $P < 0.001$). During the probe trial, IL-4$^{-/-}$ mice showed significantly reduced time spent in the training quadrant (ii), passed over the original platform location fewer times (iii), and took significantly longer to successfully locate the original platform location (iv; Student's *t* test; *, $P < 0.05$; **, $P < 0.01$; ***, $P < 0.001$). (b, e, and g) Meningeal isolates from mice were labeled for viability, CD45, singlet cells, and CD11b to allow exact comparison of cells (see Fig. 3 h for detailed gating strategy). Cells were also labeled for IL-12 and/or TNF expression. Histograms represent comparative proinflammatory cytokine production of 3×10^3 viable, CD45^{hi}, CD11b$^+$ singlet cells from each group. Numbers on the histograms indicate actual cell counts. Meningeal isolates from MWM-trained wild-type and IL-4$^{-/-}$ mice demonstrate increased production of TNF by CD11b$^+$ cells in IL-4$^{-/-}$ mice (b). FACS data shown are from one out of two independent experiments with similar results and are representative. (c) Hippocampal tissue from wild-type and IL-4$^{-/-}$ mice was compared by qRT-PCR for relative levels of TNF mRNA expression; hippocampal isolates from IL-4$^{-/-}$ mice displayed significantly higher levels of TNF mRNA. One-way ANOVA was used for statistical analysis (*, $P < 0.05$; $n = 4$ from each group; experiment was repeated two times). (d, i–iv) Lethally irradiated wild-type mice reconstituted with bone marrow from wild-type or IL-4$^{-/-}$ mice were monitored during the MWM task performance. During the acquisition (i) phase of the task, mice that had received IL-4$^{-/-}$ bone marrow took significantly longer than controls to locate the hidden platform. Two-way repeated measures ANOVA was used for statistical analysis ($n = 7$ in each group; *, $P < 0.05$; **, $P < 0.01$). During the probe trial, mice that had received IL-4$^{-/-}$ bone marrow passed over the original platform location significantly fewer times (iii) and took significantly longer to successfully locate the original platform location (iv; Student's *t* test; *, $P < 0.05$; **, $P < 0.01$). (e) Meningeal isolates were prepared from each group ($n = 4$ pooled samples), labeled as described, and analyzed by FACS. CD11b$^+$ cells from mice that received bone marrow from IL-4$^{-/-}$ mice demonstrated increased levels of IL-12 and TNF. (f, i–iv) IL-4$^{-/-}$ mice received i.p. injection of 2×10^6 T cells from wild-type mice (expressing GFP under the UBC promoter) or IL-4$^{-/-}$ mice, and were tested after 2 wk in the MWM. During the acquisition (i) phase of the task, mice that had received IL-4$^{-/-}$ T cells took significantly

intracellular cytokines. GFP$^+$ T cells expressed high levels of IL-4 and low levels of IFN-γ, whereas GFP$^-$ T cells expressed no IL-4 and high levels of IFN-γ (Fig. 4 h).

To gain insight into the possible downstream neural mechanism mediated by the meningeal cytokine milieu, we examined the effect of different cytokines and their combinations on astrocytic expression of BDNF. BDNF has been shown to be a key molecule in several learning and memory paradigms, including the MWM (Hall et al., 2000; Choy et al., 2008). It is also expressed by astrocytes and could potentially be regulated by cytokines because of the expression on astrocytes of most of the major cytokine receptors (Benveniste, 1992; Ridet et al., 1997). Primary astrocytes after 21 d in culture were treated with IL-4, TNF, IL-12, or a combination of TNF or IL-12 with IL-4, and levels of BDNF mRNA were examined using qRT-PCR. Astrocyte cultures treated with proinflammatory cytokines demonstrated reduced levels of BDNF mRNA, in line with previous findings (Aharoni et al., 2005). We additionally demonstrate that IL-4 increases BNDF mRNA levels in astrocytes (Fig. 4 i) and, surprisingly, can significantly abrogate the BDNF mRNA reduction induced by proinflammatory cytokines in primary astrocyte cultures (Fig. 4 i), suggesting that T cell–derived IL-4 could be affecting levels of parenchymal BDNF expression. Astrocytes are in close contact with "brain borders," i.e., meningeal areas, and thus could be regulated by meningeal cytokines. Confocal images represent glial fibrillary acidic protein–positive (astrocytic marker) cells expressing BDNF in close proximity to the ventricular walls and the hippocampus (Fig. 4 j). To quantify the differences in overall BDNF expression levels, we compared levels of BDNF mRNA from wild-type and IL-4$^{-/-}$ mice before and after MWM training. Although wild-type mice exhibit a significant increase in levels of BDNF mRNA after cognitive task performance (as might be expected from previously published works; Kesslak et al., 1998; Hall et al., 2000), IL-4$^{-/-}$ mice showed no increase (Fig. 4 k), suggesting that IL-4 could be critical in the maintenance of BDNF production after performance in a learning and memory task.

DISCUSSION

In this study we describe cellular and molecular mechanisms underlying T cell–mediated beneficial effects on cognitive function. We show that T cell deficiency skews meningeal myeloid immunity toward a proinflammatory phenotype. We further show that in wild-type mice, the performance of cognitive tasks leads to the accumulation of IL-4–producing (Th2) cells in the meninges. Along these lines, deficiency of T cell–derived IL-4 results in severe cognitive impairment and in a proinflammatory skewing of meningeal myeloid cell phenotype. Meningeal T cell–derived IL-4 was shown in this study to play a dual role in the maintenance of cognitive function: it antagonizes the deleterious effects of proinflammatory cytokines on astrocytes and neurons, and promotes the expression of an astroglial phenotype supportive of cognitive function (such as increased production of BDNF by astrocytes).

Although T cells have been shown to exert beneficial effects on cognitive function (Brynskikh et al., 2008), no plausible molecular mechanism has yet been offered to account for these effects. One suggestion was that T cells invade the neural parenchyma and interact directly with neurons or, alternatively, with glial cells (microglia and astrocytes), thus affecting neuronal function indirectly (Kipnis et al., 2004; Ziv et al., 2006). A major problem with this parenchymal contact–based hypothesis, however, was the conspicuous absence of T cells in the CNS parenchyma. We show in this paper that a substantial T cell response to cognitive training does indeed take place, but that it occurs in the choroid plexus, ventricular margins, and subarachnoid spaces rather than in the parenchyma. Common to these three areas is their close spatial proximity to the brain parenchyma, as well as their ability to interact with both the peripheral circulation and the CSF (Ransohoff et al., 2003; Ransohoff and Trapp, 2005; Rebenko-Moll et al., 2006).

After wild-type mice were trained in the MWM, their meningeal T cells (primarily the CD4$^+$ population) exhibited heightened activation. These findings are in line with a previous suggestion that CD4$^+$ rather than CD8$^+$ T cells participate in the regulation of neural plasticity and cognitive function

longer than wild-type T cell–injected mice to locate the hidden platform. Two-way repeated measures ANOVA was used for statistical analysis ($n = 8$ in each group; *, $P < 0.05$; **, $P < 0.01$). During the probe trial, mice that had received IL-4$^{-/-}$ T cells showed significantly reduced time spent in the training quadrant (ii), passed over the original platform location significantly fewer times (iii), and took significantly longer to successfully locate the original platform location as compared with mice receiving T cells from wild-type donors (iv; Student's *t* test; *, $P < 0.05$). (g) Meningeal isolates were prepared from each group ($n = 4$ pooled samples), labeled as described, and analyzed by FACS. CD11b$^+$ cells from mice that received IL-4$^{-/-}$ T cells mice demonstrated increased levels of IL-12 and TNF compared with wild-type T cell–injected mice. (h) Meningeal isolates from IL-4$^{-/-}$ mice that received GFP$^+$ T cells were also labeled extracellularly for CD3 and CD4, and intracellularly for IFN-γ and IL-4. GFP$^+$ (wild-type, transferred) and GFP$^-$ (endogenous) CD4$^+$ T cells were compared for expression of intracellular cytokines. GFP$^+$ T cells expressed high levels of IL-4 and low levels of IFN-γ, whereas GFP$^-$ T cells expressed no IL-4 and high levels of IFN-γ. Numbers indicate percentages. (i) Primary cultures of astrocytes from wild-type mice were treated with 10 ng/ml of various recombinant cytokines. After 8 h, mRNA was isolated from astrocyte cultures and analyzed by qRT-PCR. Relative expression of BDNF mRNA under different treatment conditions is presented. One-way ANOVA was used for statistical analysis (*, $P < 0.05$). One representative experiment out of two independently performed experiments is presented. (j) Representative confocal images of astrocytes (glial fibrillary acidic protein; GFAP) lining the borders of the brain expressing BDNF are presented. Arrows indicate examples for areas of colocalization. DG, dentate gyrus; LV, lateral ventricle; 3rdV, third ventricle. (k) Hippocampi from naive and MWM-trained wild-type and IL-4$^{-/-}$ mice were examined for BDNF expression using qRT-PCR. Relative levels of BDNF mRNA expression are presented. One-way ANOVA was used for statistical analysis (**, $P < 0.01$; $n = 4$ from each group). One representative experiment out of three independently performed experiments is presented. Error bars represent SEM.

(Ziv et al., 2006; Wolf et al., 2009). On examining cytokine expression in the meningeal T cells of our MWM-trained mice, we found that the cytokine that showed the greatest increase was IL-4. This striking Th2 skewing of the T cell phenotype pointed to a potential alternative (M2) mode of activation of meningeal myeloid cells by these T cells (Kang et al., 2008; Martinez et al., 2008; Odegaard et al., 2008). In the absence of T cells, mouse meningeal myeloid cells exhibited a skewed proinflammatory phenotype, characterized by increased production of TNF and IL-12. The proinflammatory skew of meningeal myeloid cells seen in SCID mice was reversed after injection of wild-type T cells, whereas injection of SCID mice with IL-4$^{-/-}$ T cells had no effect on the meningeal myeloid cell phenotype. Accordingly, we propose that the interaction of T cells with meningeal myeloid cells during MWM training led to modification of the inflammatory phenotype of the latter.

IL-4$^{-/-}$ mice exhibited severe cognitive impairment in the MWM task. Moreover, we found that the meningeal myeloid cells of these mice were skewed toward a proinflammatory phenotype. To substantiate the role of T cell–derived IL-4 in cognitive function and meningeal myeloid cell phenotype, we irradiated wild-type mice and injected them with wild-type or IL-4$^{-/-}$ bone marrow. 40 d after bone marrow reconstitution, we examined their performance on the MWM task. Compared with recipients of wild-type bone marrow, the MWM performance of mice that had received IL-4$^{-/-}$ bone marrow was significantly impaired. This impairment, moreover, was accompanied by a proinflammatory skewing of their meningeal myeloid cells. In line with these findings, cognitive function in IL-4$^{-/-}$ mice was restored and proinflammatory meningeal myeloid skew was ameliorated by passive transfer of CD3^{+} T cells isolated from wild-type but not from IL-4$^{-/-}$ mice. These results thus established a link between T cell–derived IL-4 and the phenotype of meningeal myeloid cells and performance in the MWM.

It has long been known that proinflammatory cytokines are detrimental to cognitive processes when they exceed their physiological concentrations (Merrill and Chen, 1991; Hauss-Wegrzyniak et al., 1998; Reichenberg et al., 2001; Monje et al., 2003; Chen et al., 2007). Numerous proinflammatory cytokines have been shown to interfere with long-term potentiation, a molecular basis for learning and memory (Bellinger et al., 1993; Curran and O'Connor, 2001; Balschun et al., 2004; Maher et al., 2005). In this paper we show that production of BDNF, a major factor in hippocampal function, is differentially regulated in astrocytes by pro- and anti-inflammatory cytokines. When astrocytes are incubated with proinflammatory cytokines, BDNF mRNA production is reduced; however, addition of IL-4 reverses this reduction. Moreover, in our in vitro studies, IL-4 directly induced BDNF mRNA production in astrocytes. In line with these findings and with previously published observations (Kesslak et al., 1998; Hall et al., 2000), BDNF expression is increased in the hippocampi of wild-type mice after cognitive training. No such up-regulation, however, was evident in IL-4$^{-/-}$ mice. Our results regarding the role of IL-4 in cognitive function are supported by a recent publication suggesting that Th2 cells play a beneficial role in Alzheimer's disease without entering CNS parenchyma (Cao et al., 2009), with an action that is B cell and antibody secretion independent. Studies using IL-4Rα floxed mice (Herbert et al., 2004) should be performed to determine whether the major targets of meningeal IL-4 are myeloid cells (for IL-4–induced regulation of their phenotype), astrocytes (for increased BDNF production and/or prevention of its decrease induced by proinflammatory factors) or both.

Although the effects of cytokines on learning and memory have been recognized for decades, research up to now has focused mainly on the effect of peripheral cytokines on brain function, or alternatively, on the effect potentiated by direct injection of cytokines into the brain parenchyma. In this study we show, for the first time, a physiological mechanism for regulation of the cytokine milieu next door to the brain parenchyma. Anatomical proximity between the hippocampus and the lateral and third ventricles further supports the importance of the cytokine content of the meningeal milieu.

Until recently, the observed increase in proinflammatory cytokine content in the CSF of patients suffering, for example, from age-related dementia, was attributed to T cell–mediated inflammation (Hasegawa et al., 2000; Sjögren et al., 2004; Abraham et al., 2008; Buchhave et al., 2008; Godbout et al., 2008). Abnormally large numbers of proinflammatory T cells, such as those seen in patients with multiple sclerosis, are indeed expected to result in a generalized proinflammatory state in the CNS and associated areas, with concomitant cognitive deterioration. Our data now demonstrate, however, that elimination of T cells from meningeal spaces will also result in a similarly skewed proinflammatory innate immune phenotype. These findings may be of relevance for clinical manifestations of cognitive disturbances related to immunosuppressive conditions.

In summary, the results of this study provide evidence for a cellular mechanism that underlies complex neuroimmune interactions affecting learning and memory. We describe a multistep and multifactorial mechanism, probably originating in the periphery, continuing to the CSF and the meningeal immune cells, and concluding with the regulation of the cytokine content of the meningeal milieu, which could in turn regulate neurotrophic factors produced by neural cells. These results represent a major paradigm shift in the understanding of the role of T cells in the maintenance of the delicate pro- and antiinflammatory balance within the meningeal milieu. Future studies will be aimed at improving our understanding of the nature of the interactions between T cells and meningeal myeloid cells that occur either via the immunological synapse or diffusible factors. It is also important to consider the development of therapeutic models based on the direct pharmaceutical modulation of meningeal myeloid cells, thereby circumventing the need for T cell perturbation and avoiding potential complications such as autoimmune disease.

MATERIALS AND METHODS

Animals

Inbred male adult (8–10-wk-old) BALB/c/BySmn, CBySmn.CB17-*Prkdc*^{scid}/J, B6.129P2-IL4^{tm1Cgn}/J, C57BL/6-Tg(UBC-GFP)30Scha/J, and C57BL/6J mice were purchased from the Jackson Laboratory. All animals were housed in temperature- and humidity-controlled rooms, maintained on a 12-h light/dark cycle (lights on at 7:00 a.m.), and age matched in each experiment. All strains were kept in identical housing conditions. The lifespan of SCID and IL-4$^{-/-}$ mice is comparable to that of wild-type mice, and there are no specific dietary or housing requirements for either mutant strain. Animal protocols were approved by the University of Virginia Institutional Animal Care and Use Committee. All procedures complied with regulations of the Institutional Animal Care and Use Committee at the University of Virginia.

Drug treatments

Anti-VLA4. A rat monoclonal antibody to mouse VLA4 (clone PS/2) was affinity purified from hybridoma supernatants and used with the permission of K. Ley (La Jolla Institute of Allergy and Immunology, San Diego, CA). Animals were given three separate injections i.p. (1.2 mg/mouse in 250 µl of 0.1 M PBS) of antibody (or an equivalent amount of rat IgG for control mice). The first dose was given 5 d before the beginning of MWM training, the second dose was given on the day before the beginning of the task, and the last injection was given after 4 d of training.

FTY720 (short term). Animals were treated daily with an oral administration (1 mg/kg in 0.1M PBS by gavage) of FTY720 (or an equivalent amount of PBS) starting 1 wk before the initiation of training in the MWM spatial learning and memory task. Animals were continued on daily oral FTY720 treatment throughout training.

FTY20 (long term). FTY720 was dissolved in drinking water (4.3×10^{-3} mg/ml); bottles were changed daily for 8 wk before and during MWM training.

T cell isolation and transfer

Lymph nodes (axillary, inguinal, superficial, and deep cervical) were harvested, mashed, and passed twice through 70-µm nylon screens. T cells were purified (enriched by negative selection) using autoMACS, a Pan T Cell Isolation Kit, and the Possel-S program (all from Miltenyi Biotec), using the negative fraction. A sample was labeled with CD3 fluorescent antibodies and analyzed by FACS for purity. Populations analyzed contained >95% CD3$^+$ T cells. T cells were counted using a hemacytometer and trypan blue. Each mouse was injected i.p. with 2×10^7 viable T cells suspended in 250 µl of 0.1 M PBS, pH 7.4.

MWM

Mice were given four trials per day, for 4 consecutive days, to find a hidden 10-cm diameter platform located 1 cm below the water surface in a pool 1 m in diameter. The water temperature was kept between 21 and 22°C. Water was made opaque with nontoxic tempera. Within the testing room, only distal visual shape and object cues were available to the mice to aid in location of the submerged platform. The BALB/c mice used in this study have poor vision and cannot fully see the shapes and objects, although they can distinguish light from darkness. In previous studies we have addressed this possible problem by using lights as visual cues, and for the visible trial we attached a glowing stick to the platform. Changing the objects on the walls to lights and adding the glowing stick significantly improves the learning ability of BALB/c mice in this task. The escape latency, i.e., the time required by the mouse to find and climb onto the platform, was recorded for up to 60 s. Each mouse was allowed to remain on the platform for 20 s and was then moved from the maze to its home cage. If the mouse did not find the platform within 60 s, it was manually placed on the platform and returned to its home cage after 20 s. The inter-trial interval for each mouse was 5 min. On day 5, the platform was removed from the pool, and each mouse was tested by a probe trial for 60 s. On days 6 and 7, the platform was placed in the quadrant opposite the original training quadrant, and the mouse was retrained for four sessions each day. On day 8 mice were introduced to the pool with a visible platform in a third quadrant, different from the first two training quadrants, and were recorded for four trials. Data were recorded using the EthoVision automated tracking system (Noldus Information Technology). Statistical analysis was performed using analysis of variance (ANOVA) and the Bonferroni post-hoc test. Groups were counterbalanced, i.e., run in alternating order on successive training days. All MWM testing was performed between 10 a.m. and 3 p.m. during the lights-on phase. All behavior experiments were performed by an experimenter blinded to the identity of experimental groups. Representative experiments are shown out of at least two to three independently performed in each case.

Fear conditioning

Training and testing were performed in two identical chambers (28 × 21 × 22 cm; Med Associates, Inc.). A video camera was positioned in front of the chambers to allow the subjects' behavior to be observed and recorded. The floor of each chamber consisted of 18 stainless steel rods (4-mm diameter) spaced 1.5 cm apart (center to center). The rods were wired to a shock generator and scrambler for the delivery of footshock. The chambers were cleaned with a 70% ethanol solution, and pans containing a thin film of the same solution were placed underneath the grid floors. Background noise (60 dB, A scale) was supplied by a fan positioned adjacent to the boxes. The mice were placed in the conditioning context for 2 min before receiving five tone (30 s, 2.8 kHz, 85 dB)/shock (2 s, 0.5 mA) pairings spaced by 1-min inter-trial intervals. 48 h later the mice received a 5-min test in the training context. Freezing was scored by an automated system during all sessions and used as an index of memory. All fear conditioning or testing was performed between 10 a.m. and 3 p.m. during the lights-on phase. The experimenter was blind to the genotype or drug status of all animals during the procedure and scoring.

Bone marrow isolation

Mice were sacrificed using CO_2 and saturated with 70% alcohol. Skin was removed from the lower part of the body. Tissue was removed from hind legs with scissors and dissected away from the body. Remaining tissue was cleaned from the tibial and femoral bones and bones were separated at the knee joint. Bone ends were cut off. Cells were forced out of bones with a stream of 0.1 M PBS, pH 7.4, containing 10% fetal calf serum using a 10-cc syringe with a 25-gauge needle. Cells were centrifuged and resuspended at a concentration of 2×10^7 cells/ml in PBS. A 200-µl cell suspension was injected into each animal i.v.

Irradiation and bone marrow replenishment

Adult wild-type C57BL/6J mice were subjected to a lethal split dose of γ irradiation (350 rad followed 48 h later by 950 rad). 3 h after the second irradiation, mice were injected with 4×10^6 bone marrow cells freshly isolated from identical wild-type mice or from IL-4$^{-/-}$ mice. After irradiation, mice were kept on drinking water fortified with sulfamethoxazole for 3 wk to limit infection.

FACS of meningeal isolates

Mice were thoroughly transcardially perfused with 0.1 M PBS, pH 7.4, for 5 min immediately after the last training trial. Heads were removed and skulls were quickly stripped of all flesh. Mandibles were next removed, as was all skull material rostral to maxillae. Surgical scissors (Fine Science Tools) were used to remove skull tops, cutting clockwise, beginning and ending inferior to the right posttympanic hook. Brains and superior skulls were immediately placed in ice-cold FACS buffer (0.1 M PBS, 1 mM EDTA, 1% BSA, pH 7.4). Meninges (dura, arachnoid, and pia mater) were carefully removed from the interior aspect of skulls and surfaces of brains with forceps (Dumont #5; Fine Science Tools). Meninges from each group (n = 4) were pooled. Meningeal tissue was gently pressed through 70-µm nylon mesh cell strainers with sterile plastic plungers (BD) to yield a single-cell suspension. Cells were centrifuged at 1,100 RPM at 4°C for 10 min, the supernatant was removed, and cells were resuspended in ice-cold FACS

buffer. Cells were stained for extracellular markers with antibodies to CD11b conjugated to FITC or PE; CD45 conjugated to allophycocyanin (APC), APC-Cy7, or efluor 450; CD3 conjugated to efluor 450, FITC, or Alexa Fluor 780; CD4 conjugated to FITC, PE, APC, or efluor 450; CD8 conjugated to FITC or PE; CD62L conjugated to PE; CD44 conjugated to FITC; CCR7 conjugated to PE-Cy7; or CD69 conjugated to PE-Cy7 or PE. Cells were stained for intracellular markers with antibodies to IL-12 conjugated to PerCP Cy5.5, TNF conjugated to PE, IL-4 conjugated to PE or PE-Cy7, or IFN-γ conjugated to PE-Cy7 (eBioscience). For IL-4 and IFN-γ staining, meningeal isolates were incubated with 10 μg/ml brefeldin A at 37°C for 5 h and labeled with the appropriate antibodies as described (eBioscience). All cells were fixed in 1% paraformaldehyde in 0.1 M PBS, pH 7.4. Fluorescence data were collected with a CyAn ADP High-Performance Flow Cytometer (Dako) and analyzed using Flowjo software (Tree Star, Inc.). To obtain equivalent and accurate cell counts, cells were gated first using the LIVE/DEAD Fixable Dead Cell Stain Kit according to the manufacturer's instructions (Invitrogen), forward versus side scatter to eliminate debris, pulse width versus area to select singlet cells, and then by appropriate markers for cell type (e.g., CD11b for myeloid-derived cells or CD3 for T cells). All histograms for CD11b cells depict comparisons of 3–10 × 10^3 cells for each sample.

CD4+ and CD8+ meningeal T cell counts by FACS

Pooled single-cell suspensions from four mice (either naive or MWM trained) were prepared and stained for the appropriate markers, as described in the previous section. Cells were collected with a high-performance flow cytometer (CyAn ADP; Beckman Coulter). Equivalent numbers of $CD45^+$ cells were used to arrive at relative $CD3^+CD4^+$ and $CD3^+CD8^+$ numbers for each pool. These counts were divided by the number of mice used to prepare the pooled sample ($n = 4$) and multiplied by the number of samples obtained for staining from each pool, thus yielding an estimate of $CD3^+CD4^+$ and $CD3^+CD8^+$ cells from each mouse meninges. Experiments were repeated three times, and groups were compared using ANOVA.

Floating section immunohistochemistry

Free-floating sections were incubated with 10% normal serum for 1 h at room temperature in TBS containing 0.3% Triton X-100, followed by incubation with appropriate dilutions of the primary antibodies for 24–48 h at 4°C in the same buffer. Sections were washed for 5 min three times at room temperature, followed by incubation with Alexa Fluor 488 or 594 chicken/goat anti–mouse/rat IgG antibodies (1:1,000; Invitrogen) for 1 h at room temperature. Sections were washed again with TBS (5 min three times) and mounted with Aqua-Mount (Lerner Laboratories) under coverslips. For examination of meningeal cells, 40-μm sections through the anterior and posterior limits of the lateral ventricle, starting at a random anterior point before the opening of the ventricle and ending at its closing, were processed and counted by two independent observers blinded to group.

Giemsa staining

20-μm frozen mounted sections were rinsed/rehydrated for 1 min in distilled water (dH_2O) at room temperature; incubated in Giemsa solution (40 drops of stock solution [Bio-Rad Laboratories] in 40 ml dH_2O) for 30 min at 60°C; dipped five times briefly in tap water at room temperature; dipped five times briefly in 1% acetic acid; dipped five times each, successively, in 70, 95, 95, and 100% ethanol; cleared for 3 min three times in xylene; and mounted and coverslipped using Cytoseal 60 (Richard Allan Scientific). Images were taken at 100, 400, and 800× and compared by a blinded observer.

Astrocyte primary culture

Mouse astrocyte cultures were prepared from 1-d-old mouse neonates as follows. Brains were excised and placed in ice-cold HBSS. Neocortical tissue was removed and minced by passage through a 5-ml plastic pipette. The cell suspension was incubated in 0.25% trypsin at 37°C for 30 min. After adding cold heat-inactivated fetal bovine serum, trypsin inhibitor, and DNase, the tissue was washed three times with cold HBSS by resuspending the tissue and pelleting in a 4°C centrifuge. To obtain a single-cell suspension, the tissue was triturated gently by pipeting through a 5-ml serological pipette 20 times and then filtered through a 40-μm filter. These mixed glial cells were cultured to 85% confluence with culture medium consisting of DMEM/F12 with 10% fetal bovine serum, 1% glutamine, 1% amphotericin B, and 1% penicillin/streptomycin in a 5% CO_2/37°C incubator before passage. To obtain purified astrocytes, flasks were rinsed with DMEM before media changes (every 2 d for the first week) to eliminate nonadherent cells. Cultures were passaged once a week at least three times before use in co-culture experiments. Cells were passaged by rinsing two times with PBS and incubated for 3 min in 2.5% trypsin-EDTA in a 5% CO_2/37°C incubator. The supernatants were collected, spun at 1,200 rpm for 5 min, and washed two times by resuspending the cells and centrifuging at 4°C. Cell pellets were resuspended in culture medium and seeded at 10^6 cells/ml onto 24-well inserts (10^6 cells/well; 1-μm Falcon; BD) or 8 × 10^6 cells/ml in a 75-ml flask. Astrocytes were incubated with the cytokines indicated in the figures at different concentrations (10 ng/ml is the most effective dose and is presented in the results) for 12 h before RNA was isolated. J. Mandell (University of Virginia, Charlottesville, VA) and his laboratory members provided us with primary astrocytes for the initial experiments.

qRT-PCR

Total cellular RNA was isolated by using Tri Reagent (Applied Biosystems) according to the manufacturer's instructions. RNA was treated with TurboDNase (Applied Biosystems) according to the manufacturer's instructions, and cDNA was obtained by using a high-capacity cDNA Archive Kit (Applied Biosystems), according to the manufacturer's instructions, using 500 ng mRNA per sample. Mice were anesthetized with nembutal and transcardially perfused with 0.1 M PBS, pH 7.4. Heads were removed immediately and kept on ice. Meninges were removed as described in FACS of meningeal isolates. Hippocampi were dissected. All dissected tissue was placed into ice-cold RNAlater (Applied Biosystems). Total hippocampal RNA was isolated using Tri Reagent and treated with DNase I (Roche), all according to the manufacturer's instructions. Using 500 ng mRNA per sample, RNA was reverse transcribed using the iScript cDNA Synthesis Kit with an iCycler and subjected to qRT-PCR using the iQ5 Real-Time Detection System (all from Bio-Rad Laboratories). Samples were used to amplify *TNF* (forward primer, 5′-TCTTCTCATTCCTGCTTGTG-3′; reverse primer, 5′-ACTTGGTGGTTTGCTACG-3′) and *BDNF* (forward primer, 5′-CGGTACAGTTGGCCTTTGGATACCG-3′; reverse primer, 5′-GTGGGTCACAGCGGCAGATA-3′). *β-glucoronidase* was used as a control for all samples (forward primer, 5′-ACCAGCCACTATCCCTAC-3′; reverse primer, 5′-ACAGACCACATCACAACC-3′), and the concentration of gene transcripts was determined relative to the concentration of *β-glucoronidase*. All primers were validated in house by analyzing product length by gel electrophoresis. Amplification of *TNF*, *BDNF*, and *β-glucoronidase* was performed in triplicate using a reaction mixture of 5 μl of synthesized cDNA product, 12 μl SYBR Green SensiMix (Quantace), primers (0.5 μl each of 10-nm stock), and 7 μl of RT-PCR–grade water (Applied Biosystems) to a total volume of 25 μl. The real-time thermocycler protocol (iQ5 Real Time Detection System) began with a single preincubation (95°C for 3 min), followed by 40 amplification cycles of 95°C for 10 s and 55°C for 30 s, with a single fluorescence reading at the end of each amplification step. Melt curves were generated for each well, and samples demonstrating melt curves indicating amplification of a nonspecific product or incorrect melt temperature were discarded.

Online supplemental material

Fig. S1 shows that peripheral lymphopenia is induced by FTY720 treatment. Fig. S2 shows impaired performance of IL-$4^{-/-}$ mice in the reverse phase of the MWM spatial learning and memory task. Fig. S3 shows no difference in brain gross histology between wild-type and IL-$4^{-/-}$ mice. Online supplemental material is available at http://www.jem.org/cgi/content/full/jem.20091419/DC1.

We thank S. Smith for editing the manuscript, Dr. B. Wiltgen for help with contextual fear conditioning experiments, Mr. P. Kennedy for technical assistance with lymphocyte enumeration, and Dr. J. Mandell and his laboratory members for providing us with primary astrocytes for the initial experiments. Special thanks to G. Wimer and B. Tomlin for excellent animal care assistance.

This work was supported in part by awards from the National Institute of Child Health and Human Development (R21HD056293) and the National Institute of Neurological Disorders and Stroke (R01NS061973) to J. Kipnis, and from the National Institute of General Medical Sciences (R01GM067958) to K.R. Lynch. N.C. Derecki was supported by a grant from the National Institutes of Health (T32HD007323).

The authors have no conflicting financial interests.

Submitted: 30 June 2009
Accepted: 1 April 2010

REFERENCES

Abraham, J., S. Jang, J.P. Godbout, J. Chen, K.W. Kelley, R. Dantzer, and R.W. Johnson. 2008. Aging sensitizes mice to behavioral deficits induced by central HIV-1 gp120. *Neurobiol. Aging*. 29:614–621. doi:10.1016/j.neurobiolaging.2006.11.002

Aharoni, R., R. Eilam, H. Domev, G. Labunskay, M. Sela, and R. Arnon. 2005. The immunomodulator glatiramer acetate augments the expression of neurotrophic factors in brains of experimental autoimmune encephalomyelitis mice. *Proc. Natl. Acad. Sci. USA*. 102:19045–19050. doi:10.1073/pnas.0509438102

Balschun, D., W. Wetzel, A. Del Rey, F. Pitossi, H. Schneider, W. Zuschratter, and H.O. Besedovsky. 2004. Interleukin-6: a cytokine to forget. *FASEB J.* 18:1788–1790.

Baune, B.T., G. Ponath, M. Rothermundt, O. Riess, H. Funke, and K. Berger. 2008. Association between genetic variants of IL-1beta, IL-6 and TNF-alpha cytokines and cognitive performance in the elderly general population of the MEMO-study. *Psychoneuroendocrinology*. 33:68–76. doi:10.1016/j.psyneuen.2007.10.002

Bechmann, I., I. Galea, and V.H. Perry. 2007. What is the blood-brain barrier (not)? *Trends Immunol.* 28:5–11. doi:10.1016/j.it.2006.11.007

Bellinger, F.P., S. Madamba, and G.R. Siggins. 1993. Interleukin 1 beta inhibits synaptic strength and long-term potentiation in the rat CA1 hippocampus. *Brain Res.* 628:227–234. doi:10.1016/0006-8993(93)90959-Q

Benveniste, E.N. 1992. Inflammatory cytokines within the central nervous system: sources, function, and mechanism of action. *Am. J. Physiol.* 263:C1–C16.

Brinkmann, V., M.D. Davis, C.E. Heise, R. Albert, S. Cottens, R. Hof, C. Bruns, E. Prieschl, T. Baumruker, P. Hiestand, et al. 2002. The immune modulator FTY720 targets sphingosine 1-phosphate receptors. *J. Biol. Chem.* 277:21453–21457. doi:10.1074/jbc.C200176200

Brynskikh, A., T. Warren, J. Zhu, and J. Kipnis. 2008. Adaptive immunity affects learning behavior in mice. *Brain Behav. Immun.* 22:861–869. doi:10.1016/j.bbi.2007.12.008

Buchhave, P., H. Zetterberg, K. Blennow, L. Minthon, S. Janciauskiene, and O. Hansson. 2008. Soluble TNF receptors are associated with Abeta metabolism and conversion to dementia in subjects with mild cognitive impairment. *Neurobiol. Aging*. 10.1016/j.neurobiolaging.2008.10.012.

Cao, C., G.W. Arendash, A. Dickson, M.B. Mamcarz, X. Lin, and D.W. Ethell. 2009. Abeta-specific Th2 cells provide cognitive and pathological benefits to Alzheimer's mice without infiltrating the CNS. *Neurobiol. Dis.* 34:63–70. doi:10.1016/j.nbd.2008.12.015

Carson, M.J., J.M. Doose, B. Melchior, C.D. Schmid, and C.C. Ploix. 2006. CNS immune privilege: hiding in plain sight. *Immunol. Rev.* 213:48–65. doi:10.1111/j.1600-065X.2006.00441.x

Chen, J., J.B. Buchanan, N.L. Sparkman, J.P. Godbout, G.G. Freund, and R.W. Johnson. 2007. Neuroinflammation and disruption in working memory in aged mice after acute stimulation of the peripheral innate immune system. *Brain Behav. Immun.* 22:301–311.

Choy, K.H., Y. de Visser, N.R. Nichols, and M. van den Buuse. 2008. Combined neonatal stress and young-adult glucocorticoid stimulation in rats reduce BDNF expression in hippocampus: effects on learning and memory. *Hippocampus*. 18:655–667. doi:10.1002/hipo.20425

Clarke, R.M., A. Lyons, F. O'Connell, B.F. Deighan, C.E. Barry, N.G. Anyakoha, A. Nicolaou, and M.A. Lynch. 2008. A pivotal role for interleukin-4 in atorvastatin-associated neuroprotection in rat brain. *J. Biol. Chem.* 283:1808–1817. doi:10.1074/jbc.M707442200

Cserr, H.F., and P.M. Knopf. 1992. Cervical lymphatics, the blood-brain barrier and the immunoreactivity of the brain: a new view. *Immunol. Today*. 13:507–512. doi:10.1016/0167-5699(92)90027-5

Curran, B., and J.J. O'Connor. 2001. The pro-inflammatory cytokine interleukin-18 impairs long-term potentiation and NMDA receptor-mediated transmission in the rat hippocampus in vitro. *Neuroscience*. 108:83–90. doi:10.1016/S0306-4522(01)00405-5

Dantzer, R. 2001. Cytokine-induced sickness behavior: mechanisms and implications. *Ann. NY Acad. Sci.* 933:222–234.

Dantzer, R., J.C. O'Connor, G.G. Freund, R.W. Johnson, and K.W. Kelley. 2008. From inflammation to sickness and depression: when the immune system subjugates the brain. *Nat. Rev. Neurosci.* 9:46–56. doi:10.1038/nrn2297

Godbout, J.P., M. Moreau, J. Lestage, J. Chen, N.L. Sparkman, J. O' Connor, N. Castanon, K.W. Kelley, R. Dantzer, and R.W. Johnson. 2008. Aging exacerbates depressive-like behavior in mice in response to activation of the peripheral innate immune system. *Neuropsychopharmacology*. 33:2341–2351. doi:10.1038/sj.npp.1301649

Griffin, A.L., H. Eichenbaum, and M.E. Hasselmo. 2007. Spatial representations of hippocampal CA1 neurons are modulated by behavioral context in a hippocampus-dependent memory task. *J. Neurosci.* 27:2416–2423. doi:10.1523/JNEUROSCI.4083-06.2007

Hall, J., K.L. Thomas, and B.J. Everitt. 2000. Rapid and selective induction of BDNF expression in the hippocampus during contextual learning. *Nat. Neurosci.* 3:533–535. doi:10.1038/75698

Hasegawa, Y., M. Sawada, N. Ozaki, T. Inagaki, and A. Suzumura. 2000. Increased soluble tumor necrosis factor receptor levels in the serum of elderly people. *Gerontology*. 46:185–188. doi:10.1159/000022157

Hauss-Wegrzyniak, B., P. Dobrzanski, J.D. Stoehr, and G.L. Wenk. 1998. Chronic neuroinflammation in rats reproduces components of the neurobiology of Alzheimer's disease. *Brain Res.* 780:294–303. doi:10.1016/S0006-8993(97)01215-8

Herbert, D.R., C. Hölscher, M. Mohrs, B. Arendse, A. Schwegmann, M. Radwanska, M. Leeto, R. Kirsch, P. Hall, H. Mossmann, et al. 2004. Alternative macrophage activation is essential for survival during schistosomiasis and downmodulates T helper 1 responses and immunopathology. *Immunity*. 20:623–635. doi:10.1016/S1074-7613(04)00107-4

Hickey, W.F. 1999. Leukocyte traffic in the central nervous system: the participants and their roles. *Semin. Immunol.* 11:125–137. doi:10.1006/smim.1999.0168

Kang, K., S.M. Reilly, V. Karabacak, M.R. Gangl, K. Fitzgerald, B. Hatano, and C.H. Lee. 2008. Adipocyte-derived Th2 cytokines and myeloid PPARdelta regulate macrophage polarization and insulin sensitivity. *Cell Metab.* 7:485–495. doi:10.1016/j.cmet.2008.04.002

Kelley, K.W., R.M. Bluthé, R. Dantzer, J.H. Zhou, W.H. Shen, R.W. Johnson, and S.R. Broussard. 2003. Cytokine-induced sickness behavior. *Brain Behav. Immun.* 17(Suppl. 1):S112–S118. doi:10.1016/S0889-1591(02)00077-6

Kesslak, J.P., V. So, J. Choi, C.W. Cotman, and F. Gomez-Pinilla. 1998. Learning upregulates brain-derived neurotrophic factor messenger ribonucleic acid: a mechanism to facilitate encoding and circuit maintenance? *Behav. Neurosci.* 112:1012–1019. doi:10.1037/0735-7044.112.4.1012

Kharel, Y., S. Lee, A.H. Snyder, S.L. Sheasley-O'Neill, M.A. Morris, Y. Setiady, R. Zhu, M.A. Zigler, T.L. Burcin, K. Ley, et al. 2005. Sphingosine kinase 2 is required for modulation of lymphocyte traffic by FTY720. *J. Biol. Chem.* 280:36865–36872. doi:10.1074/jbc.M506293200

Kipnis, J., H. Cohen, M. Cardon, Y. Ziv, and M. Schwartz. 2004. T cell deficiency leads to cognitive dysfunction: implications for therapeutic vaccination for schizophrenia and other psychiatric conditions. *Proc. Natl. Acad. Sci. USA*. 101:8180–8185. doi:10.1073/pnas.0402268101

Kivisäkk, P., D.J. Mahad, M.K. Callahan, C. Trebst, B. Tucky, T. Wei, L. Wu, E.S. Baekkevold, H. Lassmann, S.M. Staugaitis, et al. 2003. Human cerebrospinal fluid central memory CD4+ T cells: evidence for trafficking through choroid plexus and meninges via P-selectin. *Proc. Natl. Acad. Sci. USA*. 100:8389–8394. doi:10.1073/pnas.1433000100

Loane, D.J., B.F. Deighan, R.M. Clarke, R.J. Griffin, A.M. Lynch, and M.A. Lynch. 2009. Interleukin-4 mediates the neuroprotective effects of rosiglitazone in the aged brain. *Neurobiol. Aging.* 30:920–931. doi:10.1016/j.neurobiolaging.2007.09.001

Lyons, A., R.J. Griffin, C.E. Costelloe, R.M. Clarke, and M.A. Lynch. 2007. IL-4 attenuates the neuroinflammation induced by amyloid-beta in vivo and in vitro. *J. Neurochem.* 101:771–781. doi:10.1111/j.1471-4159.2006.04370.x

Maher, F.O., Y. Nolan, and M.A. Lynch. 2005. Downregulation of IL-4-induced signalling in hippocampus contributes to deficits in LTP in the aged rat. *Neurobiol. Aging.* 26:717–728. doi:10.1016/j.neurobiolaging.2004.07.002

Martinez, F.O., A. Sica, A. Mantovani, and M. Locati. 2008. Macrophage activation and polarization. *Front. Biosci.* 13:453–461. doi:10.2741/2692

McAfoose, J., H. Koerner, and B.T. Baune. 2009. The effects of TNF deficiency on age-related cognitive performance. *Psychoneuroendocrinology.* 34:615–619. doi:10.1016/j.psyneuen.2008.10.006

Merrill, J.E., and I.S. Chen. 1991. HIV-1, macrophages, glial cells, and cytokines in AIDS nervous system disease. *FASEB J.* 5:2391–2397.

Monje, M.L., H. Toda, and T.D. Palmer. 2003. Inflammatory blockade restores adult hippocampal neurogenesis. *Science.* 302:1760–1765. doi:10.1126/science.1088417

O'Keefe, J., and J. Dostrovsky. 1971. The hippocampus as a spatial map. Preliminary evidence from unit activity in the freely-moving rat. *Brain Res.* 34:171–175. doi:10.1016/0006-8993(71)90358-1

Odegaard, J.I., R.R. Ricardo-Gonzalez, A. Red Eagle, D. Vats, C.R. Morel, M.H. Goforth, V. Subramanian, L. Mukundan, A.W. Ferrante, and A. Chawla. 2008. Alternative M2 activation of Kupffer cells by PPARdelta ameliorates obesity-induced insulin resistance. *Cell Metab.* 7:496–507. doi:10.1016/j.cmet.2008.04.003

Pachter, J.S., H.E. de Vries, and Z. Fabry. 2003. The blood-brain barrier and its role in immune privilege in the central nervous system. *J. Neuropathol. Exp. Neurol.* 62:593–604.

Perry, V.H., C. Cunningham, and C. Holmes. 2007. Systemic infections and inflammation affect chronic neurodegeneration. *Nat. Rev. Immunol.* 7:161–167. doi:10.1038/nri2015

Qing, Z., D. Sewell, M. Sandor, and Z. Fabry. 2000. Antigen-specific T cell trafficking into the central nervous system. *J. Neuroimmunol.* 105:169–178. doi:10.1016/S0165-5728(99)00265-9

Ransohoff, R.M., and B.D. Trapp. 2005. Taking two TRAILS. *Neuron.* 46:355–356. doi:10.1016/j.neuron.2005.04.028

Ransohoff, R.M., P. Kivisäkk, and G. Kidd. 2003. Three or more routes for leukocyte migration into the central nervous system. *Nat. Rev. Immunol.* 3:569–581. doi:10.1038/nri1130

Rebenko-Moll, N.M., L. Liu, A. Cardona, and R.M. Ransohoff. 2006. Chemokines, mononuclear cells and the nervous system: heaven (or hell) is in the details. *Curr. Opin. Immunol.* 18:683–689. doi:10.1016/j.coi.2006.09.005

Reichenberg, A., R. Yirmiya, A. Schuld, T. Kraus, M. Haack, A. Morag, and T. Pollmächer. 2001. Cytokine-associated emotional and cognitive disturbances in humans. *Arch. Gen. Psychiatry.* 58:445–452. doi:10.1001/archpsyc.58.5.445

Ridet, J.L., S.K. Malhotra, A. Privat, and F.H. Gage. 1997. Reactive astrocytes: cellular and molecular cues to biological function. *Trends Neurosci.* 20:570–577. doi:10.1016/S0166-2236(97)01139-9

Rosicarelli, B., B. Serafini, M. Sbriccoli, M. Lu, F. Cardone, M. Pocchiari, and F. Aloisi. 2005. Migration of dendritic cells into the brain in a mouse model of prion disease. *J. Neuroimmunol.* 165:114–120. doi:10.1016/j.jneuroim.2005.04.017

Sjögren, M., S. Folkesson, K. Blennow, and E. Tarkowski. 2004. Increased intrathecal inflammatory activity in frontotemporal dementia: pathophysiological implications. *J. Neurol. Neurosurg. Psychiatry.* 75:1107–1111. doi:10.1136/jnnp.2003.019422

Sparkman, N.L., J.B. Buchanan, J.R. Heyen, J. Chen, J.L. Beverly, and R.W. Johnson. 2006. Interleukin-6 facilitates lipopolysaccharide-induced disruption in working memory and expression of other proinflammatory cytokines in hippocampal neuronal cell layers. *J. Neurosci.* 26:10709–10716. doi:10.1523/JNEUROSCI.3376-06.2006

Widner, H., G. Möller, and B.B. Johansson. 1988. Immune response in deep cervical lymph nodes and spleen in the mouse after antigen deposition in different intracerebral sites. *Scand. J. Immunol.* 28:563–571. doi:10.1111/j.1365-3083.1988.tb01488.x

Wolf, S.A., B. Steiner, A. Akpinarli, T. Kammertoens, C. Nassenstein, A. Braun, T. Blankenstein, and G. Kempermann. 2009. CD4-positive T lymphocytes provide a neuroimmunological link in the control of adult hippocampal neurogenesis. *J. Immunol.* 182:3979–3984. doi:10.4049/jimmunol.0801218

Yang, Z., M. Chen, L.B. Fialkow, J.D. Ellett, R. Wu, V. Brinkmann, J.L. Nadler, and K.R. Lynch. 2003. The immune modulator FYT720 prevents autoimmune diabetes in nonobese diabetic mice small star, filled. *Clin. Immunol.* 107:30–35. doi:10.1016/S1521-6616(02)00054-2

Yednock, T.A., C. Cannon, L.C. Fritz, F. Sanchez-Madrid, L. Steinman, and N. Karin. 1992. Prevention of experimental autoimmune encephalomyelitis by antibodies against alpha 4 beta 1 integrin. *Nature.* 356:63–66. doi:10.1038/356063a0

Ziv, Y., N. Ron, O. Butovsky, G. Landa, E. Sudai, N. Greenberg, H. Cohen, J. Kipnis, and M. Schwartz. 2006. Immune cells contribute to the maintenance of neurogenesis and spatial learning abilities in adulthood. *Nat. Neurosci.* 9:268–275. doi:10.1038/nn1629